

# From the Pendulum to Rydberg Accelerator and Planetary Dynamics: Autoresonant Formation and Control of Nonlinear States

Lazar Friedland

**Abstract**—How to excite and control a nontrivial state in a Hamiltonian system by using a perturbation and without feedback? A solution to this problem via passage through resonances and adiabatic synchronization is discussed. The idea is based on capturing the system into persistent (auto-) resonance with a chirped frequency driving perturbation such that the driving amplitude exceeds a threshold. Among other applications, this approach allows efficient control of a classical state of Rydberg atoms in 3D, yielding gradual acceleration of the electron in the atom, until approaching the stochastic ionization limit. A similar phenomenon explains the Plutino puzzle of the early evolution of the solar system.

## I. INTRODUCTION

Formation and control of nontrivial states in a nonlinear system by starting from a simple equilibrium and using a perturbation is one of the most important goals of nonlinear science. Typically, such control can be achieved by using some sort of feedback scheme (this is how we excite a child's swing, for example). However, realization of the feedback in more complex systems requires careful diagnostics of the evolving nonlinear state and becomes increasingly difficult with the increase of the number of degrees of freedom. This leads to a question of whether one can avoid feedback for controlling a system in some domain of allowed states, still using a simple controlling perturbation. Remarkably, in a large class of applications the answer to this question is positive. The idea is to exploit the salient feature of nonlinear systems to stay in resonance with driving perturbations even when the driving frequency varies in time. This self-phase-locking ability is usually referred to as the *autoresonance* phenomenon. The persistent phase-locking in the driven system is translated, under certain conditions, to a large excursion in the available solutions space. Thus, in autoresonance, the system is controlled by an oscillating perturbation simply by variation of external parameters. The autoresonance phenomenon was first used 60 years ago in applications to particle accelerators [1,2]. Only relatively recently it was identified as a general phenomenon characteristic of many nonlinear systems. First application outside accelerators field was reported by Meerson and Friedland [3], who studied autoresonant excitation of one-dimensional Rydberg atoms. Since then, similar ideas were applied in a variety of dynamical [4-10] and extended [11-17] systems. Most recent applications involve control of non-neutral plasmas

This work was supported by the Israel Science Foundation (grant No. 187/02) and INTAS (grant No.03-51-4286).

L. Friedland is with the Racah Institute of Physics, The Hebrew University of Jerusalem, Edmond Saffra Campus, Givat Ram, Jerusalem 91904, Israel; [www.phys.huji.ac.il/~lazar](http://www.phys.huji.ac.il/~lazar); [lazar@vms.huji.ac.il](mailto:lazar@vms.huji.ac.il).

vorticity dominated flows [18,19] and excitation of multiphase nonlinear waves [20,21].

This work reviews the theory of dynamic autoresonance and illustrates it in three applications. In particular, we discuss autoresonant excitation and control of a pendulum (Sec.II), manipulation of a classical state of a Rydberg atom in 3D [8] (Sec.IV), and a related Plutino problem [10] in planetary dynamics (Sec.V). All these applications involve passage through resonances and a universal threshold phenomenon for adiabatic synchronization (Sec.III).

## II. AUTORESONANTLY DRIVEN PENDULUM

We proceed from the problem of excitation of a pendulum to large energies by a perturbation and without feedback. Starting in equilibrium and slowly passing through resonance yields the solution to this problem. This is illustrated in Fig.1, where the solid line shows the evolution of the "energy"  $E = 0.5u_t^2 - \cos u + 1$  of the driven pendulum

$$u_{tt} + \sin u = \varepsilon \cos \phi_d, \quad (1)$$

where the driving phase is  $\phi_d = \int \omega(t)dt$ , while the driving frequency  $\omega(t) = 1 - \alpha t$  decreases in time, passing linear resonance at  $t=0$ . We used parameters  $\varepsilon = 0.02$ ,  $\alpha = 0.001$  and initial condition  $u = 0$  at  $t = -300$  in this simulation. One observes a continuing growth of energy in the Figure, approaching the maximum possible energy  $E = 2$  of oscillations despite the smallness of the driving amplitude. One also finds that there exists a sharp threshold on the driving amplitude (in our case  $\varepsilon_{th} = 0.0185$ ) below which the

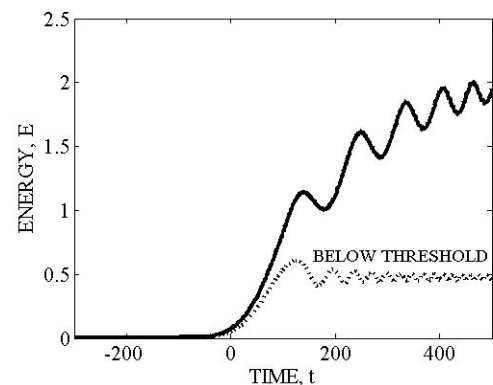


Fig.1. Autoresonantly driven pendulum. Energy versus time for driving amplitudes above (solid line) and below (dotted line) threshold.

energy saturates at a relatively low level (see the dashed line in Fig.1 for  $\varepsilon = 0.0165$ ). We shall discuss the threshold phenomenon in Sec.III.

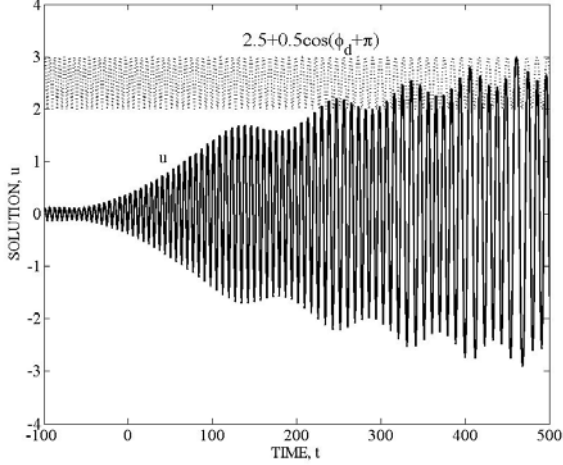


Fig.2. Adiabatic phase locking in the driven system. Solution  $u$  (solid line) and rescaled and phase shifted by  $\pi$  driving function (dotted line) versus time.

For a better understanding of the growing energy solution ( $\varepsilon > \varepsilon_{th}$ ), we show the actual evolution of  $u$  in our example in Fig.2 (solid line). In the same Figure we show function  $f(t) = 2.5 + 0.5 \cos(\phi_d + \pi)$  (dotted line) representing the driving perturbation which is scaled up in amplitude for better exposition and with the phase shifted by  $\pi$ . One observes a nearly perfect phase-locking (synchronization) in the Figure, as frequency  $\Omega$  of the pendulum follows the driving frequency despite the decrease of  $\omega(t)$  with time. At the same time the phase of the pendulum follows that of the drive shifted by  $\pi$ . This continuous phase-locking in the system constitutes the autoresonance phenomenon. The phase-locking yields a simple explanation of the observed growth of the energy of the driven system. Indeed, in autoresonance,  $\Omega(E) \approx \omega(t)$ , while  $\omega(t)$  decreases in time, and the only way for the pendulum to *decrease* its oscillation frequency is to *increase* its energy. Remarkably, in autoresonance, we approximately know the time dependence of the amplitude (energy) of the pendulum from its algebraic relation to the driving frequency, while the phase of the pendulum is nearly the same as the driving phase. Therefore we know an approximate solution of the driven problem at all times, a rare situation for a non-autonomous system.

The general theory of autoresonance in driven one-degree-of-freedom dynamical systems is developed in [13] on the bases of the Whitham's averaged variational principle [22]. This approach is equivalent to analyzing the driven problem in terms of the action-angle variables, but is more general and can be applied in studying autoresonance in extended, multidimensional systems. This theory explained most

stages of the autoresonant evolution, i.e., the initial (linear) phase locking stage prior the linear resonance, as well as weakly and strongly nonlinear stages of interaction. For example, it described the slow oscillating modulations of the energy seen in Fig.1. The frequency  $\nu$  of these oscillations scales as  $\nu \sim \varepsilon^{1/2}$ . Nevertheless, the aforementioned autoresonance threshold phenomenon was identified somewhat later in non-neutral plasma experiments [18]. In the next Section, we apply Whitham's approach in deriving a *universal* equation describing the threshold phenomenon for the pendulum and many other applications. But, prior to dealing with thresholds, we discuss another important issue associated with autoresonance, i.e. the escape from autoresonance when the driven pendulum approaches the separatrix at  $|u| \approx \pi$ . We illustrate this effect in Fig.3, showing the evolution of the energy of the pendulum for all parameters the same as in Fig.1, but for 10 different initial driving phases distributed uniformly between  $0$  and  $2\pi$ . One can see in the Figure that the evolution is similar in all runs until the pendulum reaches energy  $E \approx 1.9$  at  $t_c \approx 550$  and beyond  $t_c$  the solutions separate and become strongly dependent on the initial driving phase. In some cases the energy exceeds 2, indicating transition to rotation. This evidently chaotic behavior near separatrix is related to resonance overlap phenomenon [23] and characterizes the driven system as the frequency  $\nu$  of autoresonant modulations of energy seen in the Figure approaches some fraction ( $\sim 50\%$ ) of the decreasing frequency  $\Omega(E)$  of the pendulum.

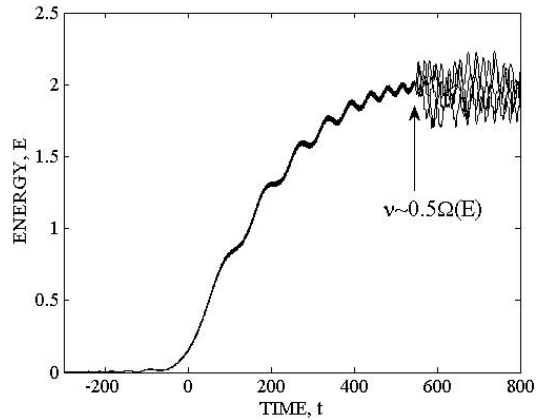


Fig.3. Autoresonant approach to stochastic instability. Energy  $E$  of the driven pendulum versus time  $t$  for 10 different initial driving phases.

### III. THE THRESHOLD PHENOMENON

The autoresonance threshold is a weakly nonlinear phenomenon, so we consider a weakly nonlinear driven pendulum problem

$$u_{tt} + u - \beta u^3 = \varepsilon \cos \phi_d, \quad \beta = 1/6. \quad (2)$$

The Lagrangian of this problem is

$$L = \frac{1}{2}(u_t^2 - u^2) + \frac{1}{4}\beta u^4 + \varepsilon u \cos \phi_d. \quad (3)$$

According to Whitham [22], we seek a two-scale representation of the driven solution, i.e.  $u = a(t) \cos \theta(t)$ , where  $\theta$  is a *fast* angle variable, while the amplitude  $a(t)$ , frequency  $\Omega = \theta_t$  and the phase mismatch  $\Phi = \theta - \phi_d + \pi$  are *slow* functions of time. We substitute this representation into the Lagrangian and average it over  $\theta$ , yielding the averaged Lagrangian

$$\Lambda(a, \theta_t, \theta) = \frac{1}{4}(\Omega^2 - 1)a^2 + \frac{3}{32}\beta a^4 - \frac{1}{2}\varepsilon a \cos \Phi. \quad (4)$$

The averaged Lagrangian yields the following evolution equations for the slow dynamical variables in the problem:

$$a_t = \frac{1}{2}\varepsilon \sin \Phi, \quad \Phi_t = \alpha t - \frac{3}{8}\beta a^2 + \frac{1}{2}(\varepsilon/a) \cos \Phi, \quad (5)$$

where we used  $\Omega^2 - 1 \approx 2(\Omega - 1)$  and  $(\phi_d)_t = \omega(t) = 1 - \alpha t$ . Finally by introducing dimensionless time  $\tau = \alpha^{1/2}t$  and driving parameter  $\mu = \frac{1}{4}(\frac{3}{2})^{1/2}\beta^{1/2}\alpha^{-3/4}\varepsilon$ , and defining a new complex dependent variable  $\Psi = \frac{1}{2}(\frac{3}{2})^{1/2}\beta^{1/2}\alpha^{-1/4}a \exp(-i\Phi)$ , we convert system (5) of real equations into a nonlinear Schrödinger-type equation

$$i\Psi_\tau + (|\Psi|^2 - \tau)\Psi = \mu, \quad (6)$$

which is fundamental to this and many other autoresonant applications. It is this *single* parameter equation which describes the threshold phenomenon in the system. Indeed, we are interested in passage through resonance, i.e., by starting from  $\Psi = 0$  at  $\tau \rightarrow -\infty$ , seek an asymptotic solution for  $\Psi$  at  $\tau \rightarrow \infty$ . One can identify two such asymptotic solutions of (6): (a) a constant amplitude (bounded) solution  $\Psi = a_0 \exp(\frac{i}{2}\tau^2)$  and (b) a growing amplitude solution,  $\Psi \sim \sqrt{\tau}$ . It is the latter, phase-locked ( $\Phi = 0$ ) solution comprises the autoresonant state in the system. Note that  $\Phi = 0$  means that the phase of the driven pendulum is the same as that of the drive shifted by  $\pi$ , as indeed can be seen in Fig.2. But how the system makes the choice between the saturated and phase-locked solutions by starting from the same (zero) initial conditions? The answer is simple: it is the parameter  $\mu$  in (6), which controls the bifurcation. Numerically, one finds that a sharp transition occurs at  $\mu > \mu_{th} = 0.41$ . By returning to our original parameters, yields the autoresonance threshold scaling of the driving amplitude

$$\varepsilon_{th} = 1.34\beta^{-1/2}\alpha^{3/4}. \quad (7)$$

Numerical simulations of the full driven system show that this result is correct in a broad range of parameters. As mentioned earlier, the sharp transition to autoresonance at  $\varepsilon_{th}$  and  $\varepsilon_{th} \sim \alpha^{3/4}$  scaling were first observed in experiments [18]. It should be mentioned that a similar theory of thresholds for capture into autoresonance can be developed for any Hamiltonian, one-degree of freedom dynamical system, which reduces to a driven Duffing oscillator in the small amplitude limit. Autoresonant vibrational excitation of diatomic molecules in 1D by chirped frequency radiation [6] is one such example. The problem of thresholds and the relation between the classical autoresonance and quantum-mechanical ladder climbing process in this case is discussed in [9]. This completes our review of 1D autoresonance and we proceed to examples of autoresonance in systems with more than one-degree of freedom.

#### IV. 3D RYDBERG ACCELERATOR

Here we address the question of how to control a classical state of the electron in a Rydberg H-atom in 3D, i.e., manipulate its energy, orbital eccentricity and inclination by a small perturbation. A similar question in 1D was studied in [3] and the term "Rydberg accelerator" to describe autoresonant excitation in this case was suggested in that work. Here we discuss a general 3D case [8] using passage through and capture into *different* resonances in the problem, the possibility arising due to a larger number of degrees of freedom. A similar theory was recently developed for control of vibrational and rotational degrees of freedom of diatomic molecules in 3D [24].

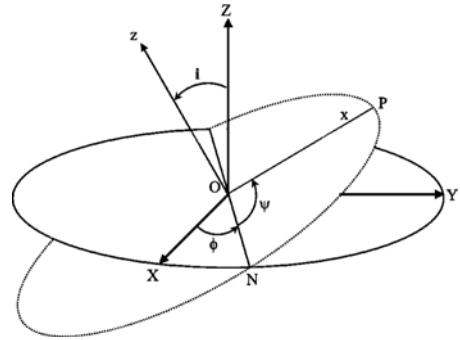


Fig.4. The Keplerian ellipse (dotted line) and Euler's angles  $\phi, \psi, i$ . The polarization of the driving electric field is in the Z direction.

We consider a classical electron in an H-atom perturbed by linearly polarized, chirped frequency oscillating electric field in the Z-direction (see Fig.4). The dynamics of the electron is governed by Hamiltonian

$$H = H_0 + \varepsilon Z \cos[\int \omega dt], \quad (8)$$

where the unperturbed part  $H_0 = \frac{1}{2}p^2 - 1/r$ . We focus on the case when the unperturbed electron starts on a circular orbit of radius  $r_0$  [angular frequency  $\Omega_0 = e(m_e r_0^3)^{-1/2}$ ] and replace  $e, m_e = 1$  in the Hamiltonian, equivalent of using dimensionless time  $t \rightarrow \Omega_0 t$ , dimensionless coordinates  $(X, Y, Z) \rightarrow (X, Y, Z)/r_0$ , radius  $r \rightarrow r/r_0$  and momentum  $p \rightarrow p/(m_e \Omega_0 r_0)$ . The dimensionless electric field amplitude in (8) is  $\varepsilon = (r_0^2/e)E_0$ . The important step in studying autoresonance in this problem is transformation to the canonical action-angle variables  $I_{1,2,3}$  and  $\theta_{1,2,3}$  of the unperturbed Hamiltonian. The normalized set of such action variables is related to different physical quantities,  $I_1 = M_z/M_0$ ,  $I_2 = M/M_0$ , and  $I_3 = (m_e e^4 / 2M_0^2 |E|)^{1/2}$ , where  $M, M_z, E$  are the angular momentum, projection of the angular momentum on the direction of polarization of the driving field and energy of the unperturbed electron respectively, while  $M_0 = m_e \Omega_0 r_0^2$  is the initial angular momentum. The formal reduction procedure to the action-angle variables is described in the classical textbook [25]. Here we shall present only the final results. One finds that the inclination angle  $i$  of the orbit, eccentricity  $e$  and normalized semi-major axis  $a$  of the orbital ellipse are simply related to the actions:  $\cos i = I_1/I_2$ ,  $e^2 = 1 - I_2^2/I_3^2$ ,  $a = I_3^2$ , while the unperturbed Hamiltonian becomes  $H_0 = -1/(2I_3^2)$ . Then (8) can be written as

$$H = -\frac{1}{2I_3^2} + \varepsilon Z(I_1, I_2, I_3, \theta_1, \theta_2, \theta_3) \cos[\int \omega dt]. \quad (9)$$

Next, we use  $2\pi$ -periodicity of coordinate  $Z$  with respect to all angle variables and expand it in Fourier series, i.e. write

$$H = -\frac{1}{2I_3^2} + \frac{1}{2}\varepsilon \sum_{k,l,m,\pm} a_{k,l,m}^\pm(I_1, I_2, I_3) e^{i(k\theta_1 + l\theta_2 + m\theta_3 \pm \int \omega dt)}. \quad (10)$$

Finally, by single resonance approximation, we neglect all terms in the perturbation in (10), but a *single* term with the choice of resonance (phase-locking) in the system. An example of a single resonance approximation in the context of autoresonant control of orbital eccentricity is described next.

We start on a circular orbit and drive the system by linearly polarized electric field having chirped frequency passing through twice the initial Keplerian frequency ( $\omega_K = 2$ ) of the atomic electron, i.e.  $\omega = 2 - \alpha t$  (the linear form of the chirp is chosen for convenience). An example of formation and growth of eccentricity with the driving field

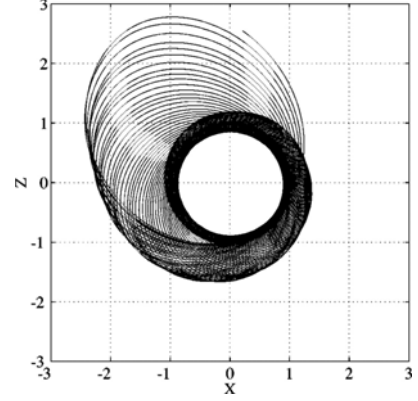


Fig.5. Autoresonant increase of orbital eccentricity of the driven electron during passage through 2:1 resonance [8].

of this form is shown in Fig.5 for drive's amplitude  $\varepsilon = 0.015$ , chirp rate  $\alpha = 0.002$  and driving field polarization in the orbital plane ( $i_0 = \pi/2$ ). The single resonance approximation in this case corresponds to leaving the term with phase factor  $2\theta_3 + \theta_2 - \int \omega dt$  only in the perturbing part in (10). Then, focusing on the case of small eccentricities, we arrive at the following single resonance Hamiltonian [8]

$$H_{sr}^j = -\frac{1}{2I_3^2} + \frac{\varepsilon e a}{4} \sin i \cos \Phi, \quad (11)$$

where  $\Phi = 2\theta_3 + \theta_2 - \int \omega dt - \pi/2$ . This Hamiltonian yields two conservation laws  $I_1 = I_{10} = \text{const}$  and  $2I_2 - I_3 = 1$ , where initially, on the circular orbit, we set  $I_{20} = I_{30} = 1$ . Thus, the problem reduces to a one-degree-of-freedom problem for, say  $I_3$  and  $\Phi$ . We write  $I_3 = 1 + \delta$ , where  $\delta$  is small. Within this approximation,  $I_2 \approx 1 + \delta/2$ ,  $e \approx \delta^{1/2}$ , and  $\sin i \approx \sin i_0$ . Then, to lowest order in  $e$ , (11) yields the following slow evolution equations for  $\delta$  and  $\Phi$

$$\begin{aligned} \delta_t &= \frac{\varepsilon \sin i_0}{2} \delta^{1/2} \sin \Phi, \\ \Phi_t &= \alpha - 6\delta + \frac{\varepsilon \sin i_0}{4\delta^{1/2}} \cos \Phi. \end{aligned} \quad (12)$$

This system, in turn, reduces to the fundamental equation (6) describing weakly nonlinear stage of autoresonance by defining  $\Psi = 6^{1/2} \alpha^{-1/4} e \exp(-i\Phi)$  and rescaling  $\tau = \alpha t^{1/2}$ , and  $\mu = \frac{6^{1/2}}{4} \alpha^{-3/4} \varepsilon \sin i_0$ . Thus, we again encounter threshold  $\mu > 0.41$  for capture into autoresonance, yielding, by returning to our original parameters, the threshold on the driving amplitude for autoresonant control of eccentricity by passage through 2:1 resonance

$$\varepsilon_{th} = \frac{0.67}{\sin i_0} \alpha^{3/4} . \quad (13)$$

Numerical simulations of the driven system agree well with this prediction.

Remarkably, as in the case of the pendulum, in autoresonance, one can specify the time evolution of the main orbital parameters algebraically. Indeed, the autoresonant solution satisfies continuing resonance relation

$$2I_3^{-3} \approx \omega(t) = 2 - \alpha t . \quad (14)$$

Therefore,  $I_3 \rightarrow \infty$  as  $\omega(t) \rightarrow 0$ , i.e. the electron energy increases and approaches ionization limit ( $H \rightarrow 0$ ), justifying the term "Rydberg accelerator" in describing the evolution. At the same time, using the conservation law,

$$e^2 = 1 - I_2^2 / I_3^2 \approx 1 - \frac{1}{4}(1/I_3 + 1)^2 , \quad (15)$$

i.e.  $e^2 \rightarrow 3/4$  as  $I_3 \rightarrow \infty$ , while

$$\cos i = I_1 / I_2 \approx 2 \cos i_0 / (1 + I_3) \rightarrow 0 . \quad (16)$$

Finally, as in the case of the driven pendulum, one encounters stochastic instability as the electron energy approaches the ionization limit. This effect is illustrated in Fig.6, showing the evolution of energy in 10 numerical simulations of the driven system with the same initial conditions, but different initial driving phases distributed uniformly between 0 and  $2\pi$ . We used  $\varepsilon = 0.013$  and driving frequency  $\omega(t) = D + (2 - D)\exp(-\alpha t/2)$ , where  $D = 0.05$  and  $\alpha = 0.005$  in these simulations.

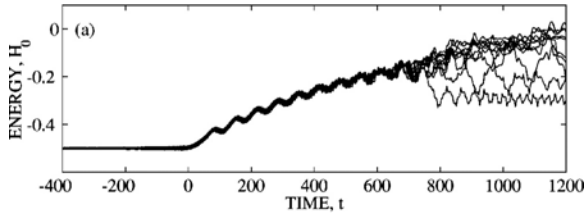


Fig.6. Autoresonant transition to stochastic instability by passage through the 2:1 resonance [8]. The electron energy  $H_0$  versus time for 10 different initial driving phases.

## V. THE PLUTINO PROBLEM

Plutinos comprise a remarkable example of autoresonance in Nature. The problem of Plutinos has features similar to those characteristic of autoresonant eccentricity control in a Rydberg atom (Sec.IV), but on a much larger (astronomical) scale of dynamics of trans-Neptunian objects in the solar system. It is known that Pluto's orbit has large eccentricity ( $e = 0.27$  on the scale between zero and one). It is also known that Pluto is in the 3:2 resonance with Neptune,

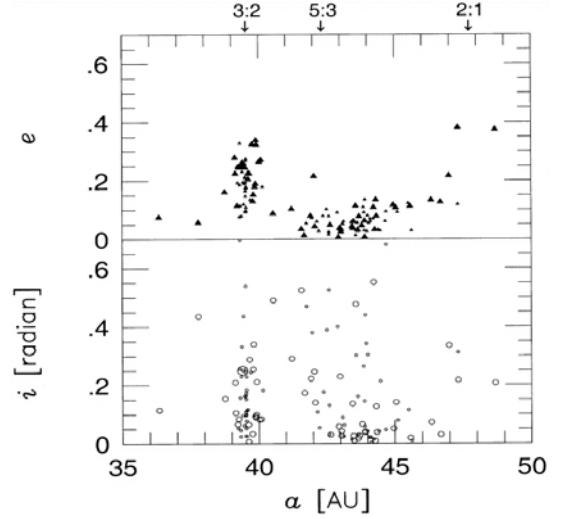


Fig. 7. Eccentricities  $e$  and inclinations  $i$  of KBOs versus semi-major axis  $a$  (from [26]). Pluto's parameters are plotted with the largest symbols. Positions of different ( $j+1$ ): $j$  resonances with Neptune are indicated at the top.

meaning that as Neptune makes three rotations around the Sun, Pluto makes two. Furthermore, Pluto is not the only trans-Neptunian object in the solar system. There exists a large number of masses (the largest known object has estimated radius of more than 1,000km) in the so called Kuiper belt beyond Neptune, and many of these masses are also in 3:2 resonance with Neptune and have large eccentricities. This is illustrated in Fig.7, showing the eccentricity of observed Kuiper Belt Objects (KBOs) as a function of the semi-major axis of their orbit [26]. Parameters of Pluto are shown in the Figure by largest symbols. One can see that in addition to Pluto there exists a large group of KBOs having similar semi-major axis, i.e., by Kepler's law, the same period of rotation around the Sun. The calculation shows that the periods of these masses are in the 3:2 ratio with that of Neptune. These resonant KBOs are called Plutinos. The questions are, why so many KBOs are in 3:2 resonance with Neptune, why they all have large eccentricities, and finally, why there are no KBOs in the neighboring 2:1 resonance (see Fig.7)?

The answer to some of these questions was suggested by Malhotra [27] using the model of migrating planets. Malhotra conjectured that at the earlier stage of evolution of the solar system, all masses including Pluto and KBOs moved on circular orbits. However, Neptune (and other giant planets) slowly migrated outwards so that the radius of its orbit slowly increased by  $\sim 20\%$  due to collisions with other masses in the protoplanetary disk. Then, during the migration, Neptune passed 3:2 resonance with Pluto and other KBOs and captured them into autoresonance. But the only way for these masses to stay in resonance as Neptune's rotation slowed down, was to increase their eccentricities. This would explain two observed facts: a large number of masses in 3:2 resonance with Neptune and their relatively large eccentricities depending on how early the object was

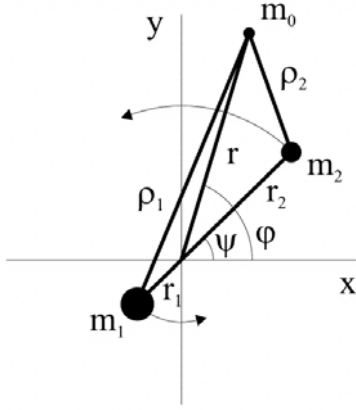


Fig.8. The geometry of the adiabatic, restricted three-body problem [10]. The masses  $m_{1,2}$  move around their center of mass on spiraling orbits having a slowly decreasing angular velocity.

trapped in resonance by the migrating planet. The only observation not explained by this theory was the small abundance of KBOs in the 2:1 resonance, which was passed by Neptune as well during its migration. In fact, in the computer simulations by Malhotra, the 2:1 resonance was populated similarly to the 3:2 resonance. A possible resolution of this puzzle was suggested recently based on the theory of thresholds for autoresonance [10]. A short description of these results is given below.

We discuss dynamics of the Sun-Neptune-Plutino system within the so called planar, *adiabatic*, restricted three-body problem illustrated in Fig.8. This model treats dynamics of a test mass  $m_0$  (Plutino) in the gravitational field of two dominant masses  $m_{1,2}$  (Sun, Neptune) rotating around their center of mass on expanding, nearly circular orbits, unperturbed by  $m_0$ . It is assumed that  $\varepsilon = m_2/m_1$  is a small parameter in the problem. The system is described by Hamiltonian

$$H = \frac{1}{2} p^2 - 1/\rho_1 - \varepsilon/\rho_2, \quad (17)$$

where we assume that the test mass moves on a circular orbit initially and use the same dimensionless momentum and radii as in the Rydberg atom problem [see definitions below (8)]. The distances  $\rho_{1,2}$  in (17) are defined as  $\rho_{1,2} = r^2 + r_{1,2}^2 \pm 2rr_{1,2} \cos \theta$ , where  $\theta = \varphi - \psi$ ,  $m_1 r_1 = m_2 r_2$ , while  $\psi(t)$  is the rotation angle of  $m_{1,2}$ , increasing with a slowly varying angular velocity  $\psi_t = \omega(t)$ . We expand  $1/\rho_1$  in (17) to first order in  $\varepsilon$ , yielding

$$H = \frac{1}{2} p^2 - 1/r + \varepsilon V_1(r, r_2, \theta). \quad (18)$$

We are interested in slow passage through a resonance in the system, fix the value of  $r_2$  in  $V_1$  at some resonance and

expand in Fourier series  $V_1 = \sum f_j(r) \cos(j\theta)$ . Finally, we transform to the canonical action-angle variables  $(I_2, I_3, \theta_2, \theta_3)$  in the problem (see a similar development in Sec.IV, but with  $I_1 = 0$  and  $\sin i = 1$  for the planar case) and make single resonance approximation in the resulting Hamiltonian, i.e. leave only one term in the Fourier series for  $V_1$ , corresponding to a particular resonance. Limiting to the case of small orbital eccentricities  $e$  of the test mass, this reduction yields the following single resonance Hamiltonian [10]

$$H_{sr}^j = -\frac{1}{2I_3^2} + \frac{\varepsilon \varepsilon a_j}{4} \cos \Phi, \quad (19)$$

where  $\Phi_j = (j+1)\theta_3 + j\theta_2 - j\psi$  and constant coefficients  $a_j$  need not be specified at the moment. We observe that this Hamiltonian is similar to that in the (planar) Rydberg atom problem [see (11)], if one sets  $j = 1$ .

Hamiltonian (19) yields a conservation law  $(j+1)I_2 - jI_3 = 1$ , where initially, on the circular orbit of the test mass, we set  $I_{20} = I_{30} = 1$ . We again write  $I_3 = 1 + \delta$ , where  $\delta$  is small in the initial excitation stage and approximate  $e \approx \delta^{1/2}$  and  $I_2 \approx 1 + j\delta/(j+1)$  from the conservation law. Then, to lowest order in  $e$ , (19) yields the following evolution equations for  $\delta$  and  $\Phi$

$$\begin{aligned} \delta_t &= \frac{(j+1)\varepsilon a_j}{4} \delta^{1/2} \sin \Phi, \\ \Phi_t &= j\alpha - 3(j+1)\delta + \frac{\varepsilon a_j}{4\delta^{1/2}} \cos \Phi. \end{aligned} \quad (20)$$

Here we have assumed passage through  $(j+1):j$ -th resonance, i.e.  $\omega(t) = (j+1)/j - \alpha t$ , with  $\alpha$  related to the slow Neptune migration rate. By rescaling  $j\alpha \rightarrow \alpha$ ,  $\frac{j+1}{2}\delta \rightarrow \delta$ , and  $\varepsilon a_j \sqrt{(j+1)/2} \rightarrow \varepsilon$ , this system reduces to (12) describing autoresonant eccentricity control in Rydberg atoms. But (12) reduces to the characteristic nonlinear Schrödinger-type equation (6), this time describing passage through a resonance in our planetary problem. Thus, we encounter the threshold on the chirp rate  $\alpha$  (in this case  $\varepsilon$  is given) for capture into  $(j+1):j$  autoresonance [compare to (13)]

$$\alpha_{th}^j = b_j \varepsilon^{4/3} \quad (21)$$

where  $b_j = (1.07/j)(j+1)^{2/3}(\varepsilon a_j)^{4/3}$ . This formula allows calculation of the shortest Neptune migration time scale  $T_j \equiv 1/\alpha_{th}^j$  for capture into  $(j+1):j$  resonance. The result

is [10]:  $T_{1,2} = 20 \times 10^6, 2 \times 10^6$  years for capture into the 2:1 and 3:2 resonances respectively. More detailed analysis shows that the order of magnitude reduction of  $T_j$  in the case of the 2:1 resonance is due to a large reduction in coefficient  $b_j$  when one includes the Sun's motion in the model, while the effect is not present in other  $(j+1):j$  resonances. Therefore, if the actual Neptune migration timescale would satisfy  $2 \times 10^6 \text{ years} < T < 20 \times 10^6 \text{ years}$ , we would observe many KBOs captured in 3:2 resonance and none in 2:1 resonance, as observed presently. Thus, we have calculated accurate bounds on Neptune's migration time scale at early stages of evolution of the solar system.

## VI. CONCLUSIONS

This paper presents a short review of dynamic autoresonance (adiabatic phase-locking) phenomenon in Hamiltonian systems. In autoresonance the system can be efficiently controlled by varying parameters of oscillating external perturbations (e.g., driving frequency) and without feedback. Passage through resonances yields a convenient approach for entering the autoresonant regime. The capture into resonance by this approach requires the driving amplitude to exceed a sharp threshold value. Typically, this threshold scales as 3/4 power of the driving frequency chirp rate. We have presented the theory of these phenomena in the case of a driven pendulum (a 1D problem), as well as in two related 3D applications, i.e. a driven Rydberg atom and the Plutino problem, occurring on vastly different space/time scales. Driving Rydberg atoms by chirped frequency radiation yields efficient control of its energy, eccentricity, and inclination. The approach also allows controlled approach to stochastic ionization as the driven electron approaches the ionization limit. In the case of Plutinos (multiple objects in the Kuiper Belt in the solar system, which all are in 3:2 resonance with Neptune), the theory of thresholds allows finding bounds on the Neptune's migration timescale in the early stages of evolution of the solar system. Studying autoresonance in dynamical systems with more than one degrees-of-freedom, as well as autoresonant manipulation and control of extended systems (waves, vortices etc.) seems to comprise important goals for future research and applications.

## REFERENCES

- [1] V.I. Veksler, "A New Method of Acceleration of Relativistic Particles," *J. Phys. USSR*, vol. 9, pp 153-158, 1945.
- [2] E.M. McMillan, "The Synchrotron-A Proposed High Energy Particle Accelerator," *Phys. Rev.*, vol. 68, pp. 143-144, 1945.
- [3] B. Meerson and L. Friedland, "Strong Autoresonance Excitation of Rydberg Atoms: The Rydberg Accelerator," *Phys. Rev. A*, Vol. 41, pp. 5233-5236, 1990.
- [4] B. Meerson and S. Yariv, "Rigid Rotator Under Slowly varying Kicks: Dynamic Autoresonance and time-varying Chaos," *Phys. Rev. A*, Vol. 44, pp. 3570-3582, 1991.
- [5] S. Yariv and L. Friedland, "Autoresonant Interaction of Three Coupled Oscillators," *Phys. Rev. E*, Vol. 48, pp. 3072-3076, 1993.
- [6] W.K. Liu, B. Wo, and J.M. Yuan, "Nonlinear Dynamics of Chirped Pulse Excitation and Dissociation of Diatomic Molecules," *Phys. Rev. Lett.*, Vol. 75, pp. 1292-1295, 1995.
- [7] L. Friedland, "Subharmonic Autoresonance," *Phys. Rev. E*, Vol. 61, pp. 3732-3735, 2000.
- [8] E. Grosfeld and L. Friedland, "Spatial Control of a Classical Electron State in a Rydberg Atom by Adiabatic Synchronization," *Phys. Rev. E*, vol. 65, pp. 046230:1-8, 2002.
- [9] G. Marcus, L. Friedland, and A. Zigler, "From Quantum Ladder Climbing to Classical Autoresonance," *Phys. Rev. A*, vol. 69, pp. 013407:1-5, 2004.
- [10] L. Friedland, "Migration Timescale Thresholds for Resonant Capture in the Plutino Problem," *Astrophys. J. A*, Vol. 547, pp. L75-L79, 2001.
- [11] M. Deutsch, B. Meerson, and J.F. Golub, "Strong Plasma Wave Excitation by a Chirped Laser Beat Wave," *Phys. Fluids B*, Vol. 3, pp. 1773-1780, 1991.
- [12] I. Aranson, B. Meerson and T. Tajima, "Excitation of solitons by an External Resonant Wave With a Slowly Varying Phase Velocity," *Phys. Rev. A*, Vol. 45, pp. 7500-7510, 1992.
- [13] L. Friedland, "Spatial Autoresonance: Enhancement of Mode Conversion Due to Nonlinear Phase-Locking," *Phys. Fluids*, Vol. B4, pp. 3199-3209, 1992.
- [14] L. Friedland, "Autoresonant Three-Wave Interactions," *Phys. Rev. Lett.*, vol. 69, pp. 1749-1752, 1992.
- [15] L. Friedland, "Autoresonant Excitation and Evolution of Nonlinear Waves: The Variational Approach," *Phys. Rev. E*, Vol. 55, pp. 1929-1939, 1997.
- [16] L. Friedland, "Resonant Excitation and Control of High Order Dispersive Nonlinear Waves," *Phys. Plasmas*, Vol. 5, pp. 645-658, 1998.
- [17] L. Friedland, "Autoresonant Solutions of Nonlinear Schrödinger Equation," *Phys. Rev. E*, Vol. 58, pp. 3865-3875, 1998.
- [18] J. Fajans. E. Gilson, and L. Friedland, "Autoresonant Excitation of the Diocotron Mode in Non-neutral Plasmas," *Phys. Rev. Lett.*, Vol. 82, pp. 4444-4447, 1999.
- [19] L. Friedland and A.G. Shagalov, "Emergence of Nonuniform V-States by Synchronization," *Phys. Fluids*, Vol. 14, pp. 3074-3086, 2002.
- [20] L. Friedland and A.G. Shagalov, "Emergence and Control of Multiphase Nonlinear Waves by Synchronization," *Phys. Rev. Lett.*, Vol. 90, pp. 074101:1-4, 2003.
- [21] L. Friedland and A.G. Shagalov, "Excitation of Multiphase Waves of Nonlinear Schrödinger Equation by Capture Into Resonances," *Phys. Rev. E*, Vol. 71, pp. 03206:1-12, 2005.
- [22] G.B. Whitham, "*Linear and Nonlinear Waves*," New York: Wiley, 1974.
- [23] B.V. Chirikov, "A Universal Instability of Many-Dimensional Oscillator Systems," *Phys. Rep.*, Vol. 52, pp. 263-379, 1979.
- [24] G. Marcus, L. Friedland, and A. Zigler, "Autoresonant Excitation and Control of Molecular Degrees of Freedom in Three Dimensions," in press, 2005.
- [25] H. Goldstein, "*Classical Mechanics*," New York: Addison-Wesley, 2<sup>nd</sup> ed., 1980.
- [26] S. Ida, G. Bryden, D.N.C. Lin, and H. Tanaka, "Orbital Migration of Neptune and Orbital Distribution of Trans-Neptunian Objects," *Astrophys. J*, Vol. 534, pp. 428-445, 2000.
- [27] R. Malhotra, *Nature*, Vol. 365, pp. 819-821, 1993.

